*Math. Model. Nat. Phenom.*
**Vol. 3, No. 2, 2008, pp. 55-74**

# Growth Constants of Unstable Surfaces in Cylindrical Systems

**L.E. Johns and R. Narayanan** [1]

Department of Chemical Engineering, University of Florida, Gainesville, FL 32611, USA

**Abstract.** We present formulas for the growth rate of surface displacements in phase change problems and flow problems in cylindrical geometries under equilibrium conditions. Our goal is to learn when domain dynamics is important vis-a-vis surface dynamics.

**Key words:** growth constants, interface instability, phase-change problems
**AMS subject classification:** 76E17

## 1 Introduction

We can identify two classes of problems where interfaces contribute to an instability. In the first class, two immiscible phases are separated by an interface. The problems in this class are flow problems, one fluid displaces the other. Typical problems are the instability of jets, of heavy fluids lying over light fluids, etc. The curvature of the interface determines local pressure variations and these translate into flows, sometimes reinforcing a displacement. The base state is an equilibrium state and cylindrical geometries give the interface two roles to play. There are two competing curvature effects: the stabilizing axial variations of the surface are accompanied by destabilizing diameter variations, viz., the diameter at a crest exceeds the diameter at a trough. These two effects alone are enough to determine the critical point of a jet. This is Rayleigh's work principle [4] explaining jet instability based on whether or not a displacement of an equilibrium jet requires work to be done. And all equilibrium cylindrical systems have in common this explanation of their critical points. Away from critical, greatest growth rates are thought to determine what is seen in an experiment.

The second class of problems are phase change problems, viz., material crosses the inter-

[1]Corresponding author. Email: ranga@ufl.edu

face. Solidification is a representative example. These are diffusion problems, ordinarily the base state is not an equilibrium state and plane interfaces have been of more interest than cylindrical interfaces.

Now equilibrium experiments are simpler to run than non-equilibrium experiments and the perturbation equations are much simpler due to the absence of base state gradients. Our goal is to see what we can learn by running the second class of problems as equilibrium, cylindrical problems.

Our plan is to present formulas for the growth rates of a variety of equilibrium systems. First we take up solidification, then electrodeposition. The first is a two phase problem, the second, one phase, but it adds in the effect of a surface reaction. These two diffusion problems are followed by flow problems, first a Darcy jet, then a Navier-Stokes jet.

In all cases we give a physical interpretation for the shape of the growth rate curves. The shapes are similar but the reasons for the shapes differ. In all these problems there are surface and bulk phase contributions to the rate of growth of a disturbance. Simple formulas obtain if the bulk dynamics is fast and can be omitted. We present physical arguments explaining whether the growth rate or its approximation should be the greater. Sometimes it is one way, sometimes the other.

# 2 Solidification

A sketch is presented as Fig. 1 showing a cylinder of radius $R_0$ in equilibrium with its melt at temperature $T_M - \dfrac{\gamma T_M}{\mathcal{L}} \dfrac{1}{R_0}$ being subjected to an axisymmetric displacement. The crests followed by troughs in the axial direction imply diameter changes in this direction and hence a doubly curved surface. The temperature rises at crests, falls at troughs, due to the diameter variation. The longitudinal curvature attempts to reverse this and at the critical point these two curvature effects are in balance. Our interest is in the growth of displacements at wave lengths greater than the critical wave length and at these wave lengths the diameter effect on the surface temperature dominates the longitudinal curvature effect.

The temperature rise at a crest leads to heat conduction away from the crest, strengthening the displacement. This effect is independent of the wave length of the disturbance. The countervailing effect, longitudinal curvature, causes the temperature at a crest to fall, leading to heat conduction into the crest, melting the crest back, weakening the displacement. This second effect depends on the wave length of the disturbance, increasing as the wave length decreases.

The formulas for the normal, twice the mean curvature and the speed of a surface, $r = R(z,t)$, are given in Fig. 1.

The surface is in equilibrium at $r = R_0$ and $T_0 = T_0^* = T_M - \dfrac{\gamma T_M}{\mathcal{L}} \dfrac{1}{R_0}$ before a displacement is imposed. The nonlinear equations, where the nonlinearity is due to the deflection of

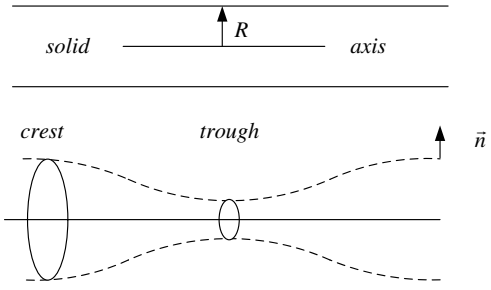


$$\vec{n} = \frac{-R_z \vec{i}_z + \vec{i}_r}{\left[1 + R_z^2\right]^{1/2}}$$

$$u = \frac{R_t}{\left[1 + R_z^2\right]^{1/2}}$$

and

$$2H = \frac{R_{zz}}{\left[1 + R_z^2\right]^{3/2}} - \frac{1}{R\left[1 + R_z^2\right]^{1/2}}$$

Figure 1: A sketch used to explain the instability of a cylindrical solid in equilibrium with its melt

the surface, are given by

$$\frac{\partial T}{\partial t} = \kappa \nabla^2 T$$

and

$$\frac{\partial T^*}{\partial t} = \kappa \nabla^2 T^*$$

on the solid and liquid domains, where the superscript $*$ denotes a liquid phase variable and where the physical properties of the two phases are taken to be the same and written as solid phase properties.

The temperatures are bounded at $r = 0$ and as $r \to \infty$ and at the surface $r = R(z,t)$ they must satisfy

$$T = T^* = T_M + \frac{\gamma T_M}{\mathcal{L}} 2H$$

where the term $\frac{\gamma T_M}{\mathcal{L}} 2H$ corrects the equilibrium temperature for the surface curvature, and

$$\lambda \vec{n} \cdot \nabla T - \lambda \vec{n} \cdot \nabla T^* = \mathcal{L} u$$

The first is the equilibrium requirement, the second is the heat balance (cf. Wollkind and Notestine [8]).

The variables $T_M$, $\lambda$, $\kappa$, $\gamma$ and $\mathcal{L}$ denote the equilibrium temperature at a plane surface, the thermal conductivity, the thermal diffusivity, the surface tension and the latent heat per unit volume.

To find the growth rate of a displacement of the surface of wave length $\frac{2\pi}{k}$, where $R = R_0 + \epsilon R_1$ and where the subscript 1 denotes a perturbation variable, we must solve

$$\frac{\partial T_1}{\partial t} = \kappa \nabla^2 T_1$$

and

$$\frac{\partial T_1^*}{\partial t} = \kappa \nabla^2 T_1^*$$

on the solid and liquid base domains subject to

$$T_1 = T_1^* = \frac{\gamma T_M}{\mathcal{L}} 2H_1$$

and

$$\lambda \frac{\partial T_1}{\partial r} - \lambda \frac{\partial T_1^*}{\partial r} = \mathcal{L} u_1$$

at $r = R_0$ where

$$u_1 = \frac{\partial R_1}{\partial t}$$

and

$$2H_1 = \frac{R_1}{R_0^2} + \frac{\partial^2 R_1}{\partial z^2}$$

Solving these equations by writing

$$T_1 = \hat{T}_1(r)\cos kze^{\sigma t}$$

$$T_1^* = \hat{T}_1^*(r)\cos kze^{\sigma t}$$

and

$$R_1 = \hat{R}_1\cos kze^{\sigma t}$$

we derive an implicit formula for the growth rate of the displacement. It is

$$\frac{\sigma R_0^2}{\kappa} = \frac{L_{cap}}{R_0}\left[1-x^2\right]\left[\frac{yI_0^{'}(y)}{I_0(y)} - \frac{yK_0^{'}(y)}{K_0(y)}\right]$$

where $K_0(y)I_0^{'}(y) - I_0(y)K_0^{'}(y) = \dfrac{1}{y}$, where

$$x = kR_0$$

$$y^2 = x^2 + \frac{\sigma}{\kappa}R_0^2$$

and where

$$L_{cap} = \frac{\gamma}{\mathcal{L}}\frac{T_M}{\mathcal{L}\kappa/\lambda}$$

Our interest is in $\dfrac{\sigma R_0^2}{\kappa}$ as a function of $x$ on the interval $0 < x < 1$, where there is one positive growth constant, the growth constant that would be of interest in a experiment on the breakup of a solid cylinder.

If the domain dynamics plays no role, i.e., if the time derivatives appearing in the domain equations are dropped, we obtain a value of $\sigma$, denoted $\sigma_s$, due entirely to what is going on at the surface. It is given by

$$\frac{\sigma_S R_0^2}{\kappa} = \frac{L_{cap}}{R_0}\left[1-x^2\right]\left[\frac{xI_0^{'}(x)}{I_0(x)} - \frac{xK_0^{'}(x)}{K_0(x)}\right]$$

Graphs of $\dfrac{\sigma R_0^2}{\kappa}$ and $\dfrac{\sigma_S R_0^2}{\kappa}$ vs $x$ at values of $\dfrac{L_{cap}}{R_0}$ where differences are apparent are presented in Fig. 2. Experiments are commonly run using succinonitrile. Its properties are given in Table 1.

We begin by stating the following conclusions

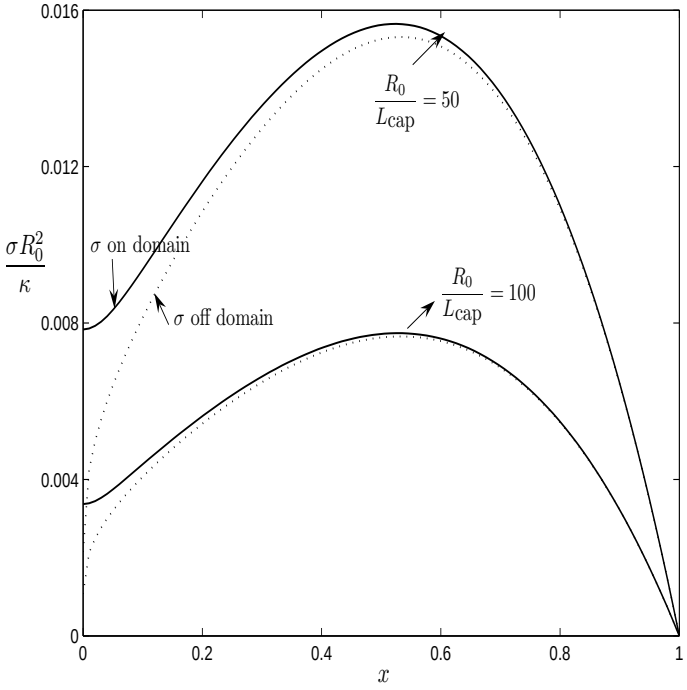


Figure 2: Growth constants in pure solidification

- The formula for $\sigma_S$ is explicit
- Dropping $\sigma$ on the domain gives a good approximation to $\sigma$, getting better as $L_{cap}/R_0$ decreases. The error is largest as $x$ approaches zero at any $L_{cap}/R_0$ but good accuracy obtains where $\sigma$ is greatest.
- The approximation is less than $\sigma$ for this and for other phase change problems
- The growth constant, $\sigma$, does not rise from zero as its approximation does. But both $\sigma$ and $\sigma_S$ rise as $x$ increases from zero, a necessary condition for a greatest growth rate to be found.
- In the region where $\sigma$ and $\sigma_S$ rise the melt controls the rate of growth, the solid is not important, i.e., the term $\frac{xI_0'(x)}{I_0(x)}$ is negligible.

To give a physical explanation for these observations imagine a solid rod of radius $R_0$ subjected to a periodic displacement of its surface. The larger diameter at a crest raises the temperature above the equilibrium value, the smaller diameter at a trough lowers the temperature. The effect due to the longitudinal curvature is the opposite. For values of $x$ less than one the diameter effect rules, more so as $x$ approaches zero. Heat is then conducted away

Table 1: Properties of succinonitrile and succinonitrile-acetone alloy

| | |
|---|---|
| Melting Point, $T_M$ | 330 (K) |
| Thermal Conductivity of solid, $k_{cond}$ | 0.23 (W/m K) |
| Thermal Diffusivity of solid, $\kappa$ | $1.2 \times 10^{-7}$ ($m^2$/s) |
| Surface Tension, $\gamma$ | $9 \times 10^{-3}$ (J/$m^2$) |
| Latent Heat of Fusion, $\mathcal{L}$ | $0.5 \times 10^{8}$ (J/$m^3$) |
| Equilibrium Distribution Coefficient, $k_{dist}$ | 0.1 (mol%/mol%) |
| Liquidus Slope, $m$ | $-2.$ (K/mol% ) |
| Liquid Mass Diffusivity, $D^*$ | $1.3 \times 10^{-9}$ ($m^2$/s) |

from the crest reinforcing the displacement. Dropping $\sigma$ on the domain allows the gradients in the surrounding solid and liquid to equilibrate instantly to the surface conditions, retaining $\sigma$ on the domain slows this accommodation implying that the sharp gradients attending the displacement tend to persist with the result that $\sigma$ is always larger than $\sigma_S$.

Turning to the rise in $\sigma$ and $\sigma_S$ as $x$ increases from zero, we notice first that this is not due to axial conduction from crest to trough. This effect does not appear in the perturbation of an equilibrium problem. The diameter effect on the surface temperatures is independent of $x$ but the depth of penetration of the induced gradients decreases as $x$ increases strengthening these gradients thereby increasing $\sigma$ and $\sigma_S$. As $x$ continues to increase, the stabilizing effect of the longitudinal curvature comes into play until it offsets the diameter effect at the critical point. We see that $\sigma$ increases from a finite value at $x = 0$ whereas $\sigma_S$ increases from zero. The instability at $x = 0$ is due to the fact that an imposed gradient remains in the surroundings so long as $\sigma$ is retained on the domain, it is eliminated if $\sigma$ is dropped on the domain, the more so the greater the depth of penetration, i.e., the smaller $x$.

To account for the presence of a dilute solute, we use the model of Mullins and Sekerka (1964) [3] whereupon the temperature problem is as above except that a term must be added to account for the lowering of the equilibrium temperature due to the presence of the solute and hence, in addition to the Gibbs-Thomson correction, we have

$$T = T^* = T_M + \frac{\gamma T_M}{\mathcal{L}} 2H + mC^*$$

where $m$ denotes the slope of the liquidus line.

The solute concentration then satisfies

$$\frac{\partial C}{\partial t} = D\nabla^2 C \quad \text{and} \quad \frac{\partial C^*}{\partial t} = D^*\nabla^2 C^*$$

on the solid and liquid domains and

$$D\vec{n} \cdot \nabla C - D^*\vec{n} \cdot \nabla C = -[C - C^*]u$$

and

$$C = kC^*$$

at the solid-melt surface where $k$ denotes the equilibrium distribution ratio.

A cylindrical solid rod of radius $R_0$, concentration $C_0$ and temperature $T_0$ in equilibrium with its melt at concentration $C_0^*$ and temperature $T_0^* = T_0 = T_M = -\frac{\gamma T_M}{\mathcal{L}}\frac{1}{R_0} + mC_0^*$ is upset by a perturbation of wave length $\frac{2\pi}{k}$. Solving the perturbation eigenvalue problem gives the growth rate of this disturbance and we have

$$\frac{\sigma R_0^2}{\kappa} = \frac{\frac{L_{cap}}{R_0}\left[1-x^2\right]\left[\frac{yI_0'(y)}{I_0(y)} - \frac{yK_0'(y)}{K_0(y)}\right]}{1 + \frac{\lambda}{\mathcal{L}}\left[\frac{m[k-1]C_0^*}{D^*}\right]\frac{\left[\frac{yI_0'(y)}{I_0(y)} - \frac{yK_0'(y)}{K_0(y)}\right]}{\left[\frac{zI_0'(z)}{I_0(z)} - \frac{zK_0'(z)}{K_0(z)}\right]}}$$

where $x$, $y$ and $z$ are given by

$$x = kR_0, \quad y^2 = x^2 + \frac{\sigma R_0^2}{\kappa}, \quad z^2 = x^2 + \frac{\sigma R_0^2}{D^*}$$

and $D$ has been set equal to $D^*$.

Upon dropping the three domain $\sigma$'s, retaining only the two surface $\sigma$'s, the corresponding result is

$$\frac{\sigma_S R_0^2}{\kappa} = \frac{\frac{L_{cap}}{R_0}\left[1-x^2\right]\left[x\frac{I_0'(x)}{I_0(x)} - x\frac{K_0'(x)}{K_0(x)}\right]}{1 + \frac{\lambda}{\mathcal{L}}\left[\frac{m[k-1]C_0^*}{D^*}\right]}$$

To illustrate the effect of adding solute, we present Fig. 3. It is drawn at a value of $\frac{L_{cap}}{R_0}$ seen earlier in the pure solidification problem.

The addition of solute slows the growth rates.The approximation is now not as good as it was before solute was added and the wave length at the greatest growth rate predicted by $\sigma_S$ is shifted maybe 10% to the right of that predicted by $\sigma$.

All the qualitative aspects of the curves remain as they were and the explanations given do not change.

The $\sigma' s$ are scaled as they were before solute was added, i.e., as though heat conduction was the controlling diffusive process. Once solute is introduced, solute diffusion becomes the controlling diffusive step and the growth rates in the same scaling are reduced.

# 3 Electrodeposition

In the simplest example of electrodeposition, two solid electrodes, eg., copper electrodes, are separated by an ionic solution, eg., copper sulphate dissolved in water. The solute ionizes

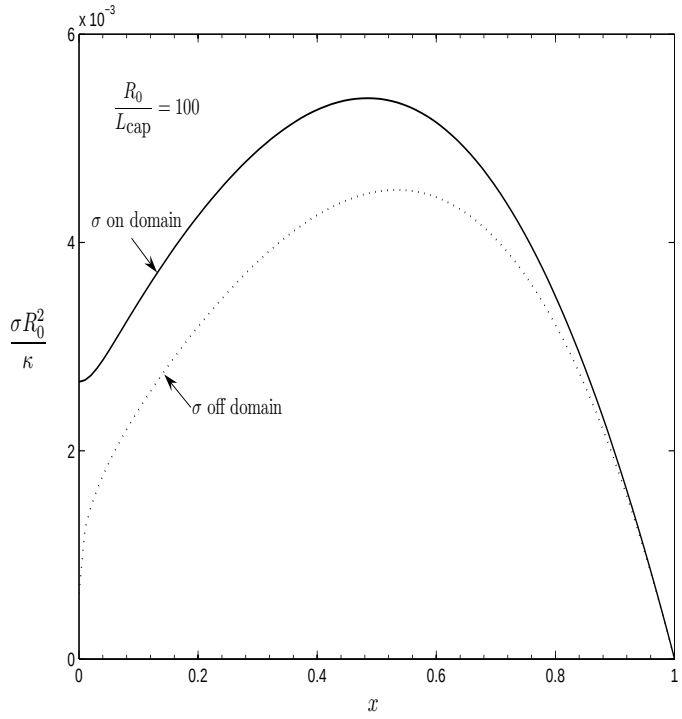


Figure 3: Growth constants in solidification-solute added

completely producing a solution containing positive and negative ions. An electron transfer reaction takes place at the electrode surfaces whereby copper ions deposit as copper metal, the reduction reaction. Its reverse also occurs whereby copper metal dissolves producing copper ions. The rate of the reduction reaction depends on the concentration of copper ions at the surface and the rates of both reactions depend on the electrical environment at the surface, viz., the difference between the electrical potential of the electrode and the electrical potential of the nearby solution.

The curvature of the electrode surface comes into play due to its influence on the energetics of the two reactions. A crest projecting into the solution, imposed on a plane electrode surface, favors oxidation over reduction, dissolving the crest and is therefore stabilizing. Displacing a cylindrical electrode surface creating crests and troughs in the axial direction leads to a curvature effect like that on a plane surface, but there is also the diameter effect which opposes this. Hence cylindrical electrodes present us with a way of obtaining information from equilibrium experiments without the need to add the complications attending steady growth experiments.

The reaction sets electrodeposition apart from solidification, otherwise the diffusion of copper ions in the solution acts like the conduction of heat in solidification. The only additional complication is that the diffusional movement of copper ions is abetted by their

migration under electrical potential gradients in the solution.

Hence there are three solution phase variables appearing in our model, the concentrations of the two ions and the electrical potential. This can be reduced to two by introducing the assumption that the solution is electrically neutral. This assumption that the charge density of the solution vanishes reduces the independent ion concentration variables to one, denoted $C$. Then in terms of $C$ and $\phi$, the electrical potential, we have, on the solution domain

$$\frac{\partial C}{\partial t} = D\nabla^2 C$$

$$P\nabla^2 C + \frac{z_1 F}{RT}\nabla \cdot C\phi = 0$$

where

$$D = \frac{D_1 D_2 \left[z_1 - z_2\right]}{z_1 D_1 - z_2 D_2}$$

and

$$P = \frac{z_1 \left[D_1 - D_2\right]}{z_1 D_1 - z_2 D_2}$$

At an electrode-solution interface we have

$$D\vec{n} \cdot \nabla C = \frac{z_1 z_2}{z_1 D_1 - z_2 D_2} D_2 C_M u$$

and

$$\frac{z_1 F}{RT} C\vec{n} \cdot \nabla\phi = -\frac{z_1}{z_2}\vec{n} \cdot \nabla C$$

where the rate of reaction at the surface is given in terms of the electrical potential at the electrode, denoted $V$, by the Butler-Volmer equation, viz.,

$$-F z_1 C_M u = i_0 \left[ e^{[1-\beta]\frac{z_1 F}{RT}\left[V-\phi-\Delta_{ref}-\frac{\gamma}{z_1 F C_M}2H\right]} - \frac{C}{C_{ref}} e^{-\beta\frac{z_1 F}{RT}\left[V-\phi-\Delta_{ref}-\frac{\gamma}{z_1 F C_M}2H\right]} \right]$$

The basis of electrodeposition can be found in Bockris and Reddy [1] and this model can be found in Sundström and Bark [5].

We begin with a cylindrical electrode of radius $R_0$ in equilibrium with a electrolytic solution at uniform ion concentration $C_0$ and electrical potential $\phi_0$. The electrical potential of the electrode, $V_0$, is then given by

$$e^{\frac{z_1 F}{RT}\left[V_0-\phi_0-\Delta_{ref}+\frac{\gamma}{z_1 F C_M}\frac{1}{R_0}\right]} = \frac{C_0}{C_{ref}}$$

Table 2: Properties of Typical of a Copper Electrode and a Copper-Sulphate Solution

| | |
|---|---|
| Molar Density of Copper, $c_M$ | 150 (kg mol/m$^3$) |
| Interfacial Tension, $\gamma$ | 1.5 (J/m$^2$) |
| Diffusion Coefficient of Cupric Ions, $D_1$ | $7 \times 10^{-10}$ (m$^2$/s) |
| Diffusion coefficient of Sulphate Ions, $D_2$ | $10^{-9}$ (m$^2$/s) |
| Exchange Current Density, $i_o$ (A/m$^2$) | 10 for $c_{ref} = 0.1$ (kg mol/m$^3$)<br>3.2 for $c_{ref} = 0.01$ |
| Symmetry Factor $\beta$ | 1/2 |

An axisymmetric displacement is imposed on the electrode surface and its growth rate obtains by solving the perturbation equations. The growth rate of a disturbance of wave length $\frac{2\pi}{k}$ is then obtained by

$$\frac{\sigma R_0^2}{D} = \frac{\frac{L_{cap}}{R_0}(1-x^2)\frac{xK_1(x)}{K_0(x)}}{1 + \frac{L_I}{R_0}\frac{xK_1(x)}{K_0(x)} + \frac{z_1 z_2 D_2}{z_1 D_1 - z_2 D_2}\frac{\left\{\frac{K_0(x)}{xK_1(x)} - \frac{K_0(y)}{yK_1(y)}\right\}}{\frac{K_0(x)}{xK_1(x)}}}$$

which becomes, on dropping domain dynamics,

$$\frac{\sigma_S R_0^2}{D} = \frac{\frac{L_{cap}}{R_0}(1-x^2)\frac{xK_1(x)}{K_0(x)}}{1 + \frac{L_I}{R_0}\frac{xK_1(x)}{K_0(x)}}$$

where $L_{cap}$ and $L_I$ are given by

$$L_{cap} = \frac{\gamma}{RTC_M}\frac{D_1}{D}\frac{C_0}{C_M}\frac{1}{z_1}$$

and

$$L_I = \frac{FC_0 D_1}{i_0}$$

The curves illustrating the dependence of $\sigma$ and $\sigma_S$ on wave number are presented in Figs. 4a and 4b. The curves are drawn for copper-copper sulfate solution where the difference first becomes apparent and then for a reaction about ten times slower. The properties of the the copper-copper sulfate solution are given in Table 2.

Qualitatively electrodeposition differs from solidification in only one way. In this case both $\sigma$ and $\sigma_S$ approach zero as $x$ approaches zero whereas in solidification $\sigma$ did not approach

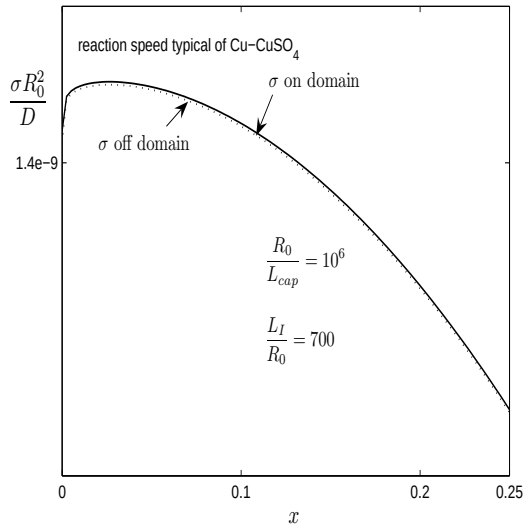


(a)

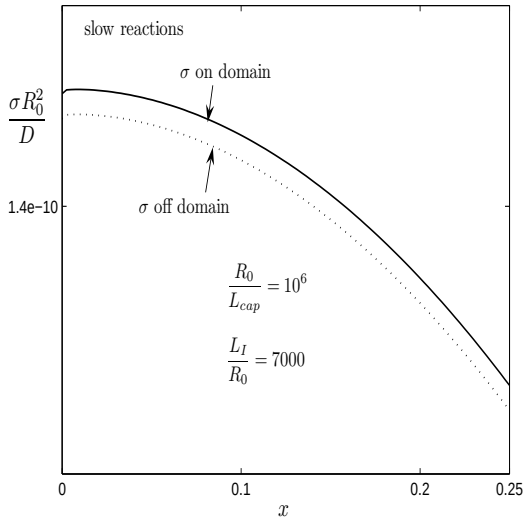


(b)

Figure 4: Growth constants for electrodeposition a) typical reaction rates b) slow reaction rates

zero. This is due to the effect of the solution electrical potential which has an effect on the rate of reaction independent of the solute concentration. If the presence of $\phi$ in the Butler-Volmer equation were omitted $\sigma$ could not vanish as $x$ goes to zero and the reason would be the same as that given in solidification. To explain this we observe first that there is no dynamics in the domain $\phi$ equation other than what is inherited through $C$. Second, at long wave lengths and vanishing gradients the concentration perturbation must vanish, but this is acceptable in electrodeposition, though not in solidification, for the displaced cylinder, at long wave lengths, can remain in equilibrium with $\phi_1$ offsetting $R_1$. Like pressure in flow problems, which also does not have its own dynamics, equilibrium solutions can be found in electrodeposition where $\phi_1$ assumes a constant value.

The effect of $i_0$ on the growth rate is strong. Fig. 4a is drawn for a value of $i_0$ typical of a dilute copper-copper sulphate solution. Figure 5 is drawn assuming the reaction is so fast that it is always in equilibrium. Also on this figure is a curve for the case where $i_0$ is 100 times the copper-copper sulphate value. As $i_0$ increases the growth rates increase and the wave number at the greatest value shifts to the right.

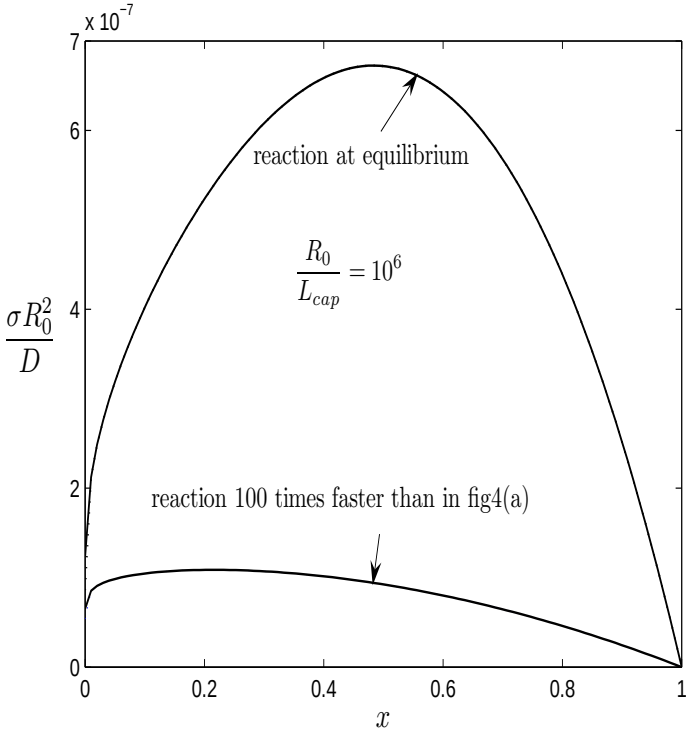


Figure 5: Growth rates in electrodeposition for reaction equilibrium and for fast surface reactions

Now an electrolytic cell must have two electrodes and hence we must have a second cylindrical electrode, concentric to the first at a radius $R_0^*$. Adding a second electrode leads

Table 3: $\sigma_{in}/\sigma_s$ for various $\eta$, $\frac{\mathrm{L_I}}{R_0}$ and wave numbers

| | $x = 0.1$ | | $x = 0.5$ | |
|---|---|---|---|---|
| $\frac{\mathrm{L_I}}{R_0}$ | $\eta = 1.1$ | $\eta = 2.0$ | $\eta = 1.1$ | $\eta = 2.0$ |
| 7000 (slow reaction) | 0.99 | 1.0 | 0.99 | 1.0 |
| 700 (reaction speed typical of Cu-$CuSO_4$) | 0.88 | 0.99 | 0.97 | 0.99 |
| 70 (fast reaction) | 0.4 | 0.95 | 0.8 | 0.99 |

to a quadratic formula for $\sigma_S$. We give the result for $\sigma_S$ which is a good approximation to $\sigma$ in electrodeposition. It is

$$(\sigma_s - \sigma_{\mathrm{in}})(\sigma_s - \sigma_{\mathrm{out}}) - \frac{T_1^* T_2}{T_1 T_2^*} \frac{1}{[\frac{\mathrm{L_I}}{R_0 T_2^*} + 1]} \frac{1}{[\frac{\mathrm{L_I}}{R_0 T_1} + 1]} \tag{3.1}$$

where

$$\sigma_{in} = \frac{\frac{\mathrm{L_{cap}}}{R_0}(1 - x^2)\frac{1}{T_1}}{[\frac{\mathrm{L_I}}{R_0 T_1} + 1]} \tag{3.2}$$

and

$$\sigma_{out} = \frac{\frac{\mathrm{L_{cap}}}{R_0}\frac{(1-\eta^2 x^2)}{\eta^2}\frac{1}{T_2^*}}{[\frac{\mathrm{L_I}}{R_0 T_2^*} + 1]} \tag{3.3}$$

and where

$$T_1 = \frac{I_0(x)K_1(\eta x) + K_0(x)I_1(\eta x)}{x[I_1(\eta x)K_1(x) - I_1(x)K_1(\eta x)]} \tag{3.4}$$

$$T_2 = -\frac{1}{x^2[I_1(\eta x)K_1(x) - I_1(x)K_1(\eta x)]} \tag{3.5}$$

$$T_1^* = \frac{1}{\eta x^2[I_1(\eta x)K_1(x) - I_1(x)K_1(\eta x)]} \tag{3.6}$$

and

$$T_2^* = -\frac{[I_0(\eta x)K_1(x) + K_0(\eta x)I_1(x)]}{x[I_1(\eta x)K_1(x) - I_1(x)K_1(\eta x)]} \tag{3.7}$$

As $\eta = \dfrac{R_0^*}{R_0}$ goes to infinity, $\sigma_{in}$ goes to our one electrode formula for $\sigma_S$, while $\sigma_{out}$ goes to the corresponding formula for a plane electrode. We give the ratio of $\sigma_{in}$ to $\sigma_S$ for one

electrode as a function of $\frac{L_I}{R_0}$, $\eta$ and a few values of $x$ in Table 3. Except for very small values of $x$ a single electrode in an infinite electrolytic solution is a very good approximation.

# 4 Jets

The problem of the stability of jets is, willy-nilly, an equilibrium problem. A cylinder of radius $R_0$ of a liquid of viscosity $\mu$ and density $\rho$ is at rest in a second fluid of viscosity $\mu^*$ and density $\rho^*$ whereupon a perturbation is given and the initial growth rate leading to breakup is of interest. This is an old problem and much is known about it [cf., Rayleigh [4] and Chandrasekhar (1960)] [2], yet some results remain to be explained, among the oddest being that when $\mu > 0$, $\mu^* = 0$ and when $\mu = 0$, $\mu^* > 0$ the greatest growth rate occurs at infinite wave length, yet when $\mu > 0$, $\mu^* > 0$ the greatest growth rate occurs at a finite wave length. These results have been obtained on assuming $\rho = 0 = \rho^*$.

Not much needs to be explained here. Crests grow due to flow toward them in the jet and away from them in the surrounding fluid. Curved surfaces induce pressure differences and pressure gradients cause flow. The axisymmetric displacement of a cylindrical surface leads to two curvatures having opposing effects on the stability of a crest.

To make the simplest departure from the diffusion problems presented in the foregoing, we take up first the Darcy jet, a problem having no inertia. Our equations are

$$\frac{\mu}{K}\vec{v} = -\nabla p$$

$$\frac{\mu^*}{K}\vec{v}^* = -\nabla p^*$$

and

$$\nabla \cdot \vec{v} = 0 = \nabla \cdot \vec{v}^*$$

in the jet and in the surrounding fluid where $K$ denotes the permeability of the medium.

At the surface of the jet we have

$$\vec{n} \cdot \vec{v} = u = \vec{n} \cdot \vec{v}^*$$

and

$$p - p^* = -\gamma 2H$$

A jet at rest of radius $R_0$ is given a small perturbation of wavelength $\frac{2\pi}{k}$.

In the case $\mu = \mu^*$ and $\rho = \rho^*$, the growth rate is given by

$$\frac{\sigma R_0^2}{\nu} = \left( \frac{R_0^2/\nu}{\frac{\mu R_0}{\gamma}} \right) \left( \frac{K}{R_0^2} \right) \frac{(1-x^2)}{\left[ \frac{I_0(x)}{xI_1(x)} + \frac{K_0(x)}{xK_1(x)} \right]}$$

We observe that $\sigma$ here is really $\sigma_S$, there being no domain dynamics in this problem and we find that $\sigma$ goes to zero as $x$ goes to zero.

This formula highlights one important difference between flow and diffusion problems: on the rising branch of the $\sigma$ vs $k$ curve, the surroundings control in diffusion problems, the cylinder controls in flow problems. This difference will be seen again in the Navier-Stokes jet.

Turning to an equilibrium thread of viscous liquid, our model will consist of the Navier-Stokes equation for the divergence free velocity in both phases, boundedness at infinity and along the axis of the cylinder and at the surface we have equality of tangential velocity and tangential stress, equality of normal velocity, equal to the normal speed of the surface and a normal stress difference arising due to the surface curvature.

We give the formulas for $\sigma$ and $\sigma_S$ in the special case, $\mu = \mu^*$, $\rho = \rho^*$ where $\rho$ and $\rho^*$ are set to zero in the formula for $\sigma_S$. These formulas are

$$\frac{\sigma R_0^2}{\nu} = \left( \frac{R_0^2/\nu}{\frac{\mu R_0}{\gamma}} \right) (1-x^2) \frac{\left[ 1 - \frac{\left( \frac{xI_1'(x)}{I_1(x)} - \frac{xK_1'(x)}{K_1(x)} \right)}{\left( \frac{yI_1'(y)}{I_1(y)} - \frac{yK_1'(y)}{K_1(y)} \right)} \right]}{(y^2-x^2) \left[ \frac{I_0(x)}{xI_1(x)} + \frac{K_0(x)}{xK_1(x)} \right]}$$

and

$$\frac{\sigma_S R_0^2}{\nu} = \frac{1}{2} \left( \frac{R_0^2/\nu}{\frac{\mu R_0}{\gamma}} \right) [1-x^2] \frac{[-2K_1(x)I_1(x) - xK_0(x)I_1(x) + xI_0(x)K_1(x)]}{xK_1(x)I_0(x) + xK_0(x)I_1(x)}$$

and graphs are presented in Fig. 6 for two values of $\frac{R_0^2/\nu}{\frac{\mu R_0}{\gamma}}$, the ratio of a diffusion time to a capillary time.

We see no reason to present the corresponding formulas when $\mu \neq \mu^*$ and/or $\rho \neq \rho^*$. They can be obtained but they are not very simple.

These graphs lead us to conclude: First, that $\sigma_S$ is a good approximation to $\sigma$; better as $\frac{R_0^2/\nu}{\mu R_0/\gamma}$ decreases and we note that the formula for $\sigma_S$ is explicit. Second, $\sigma$ and $\sigma_S$ both

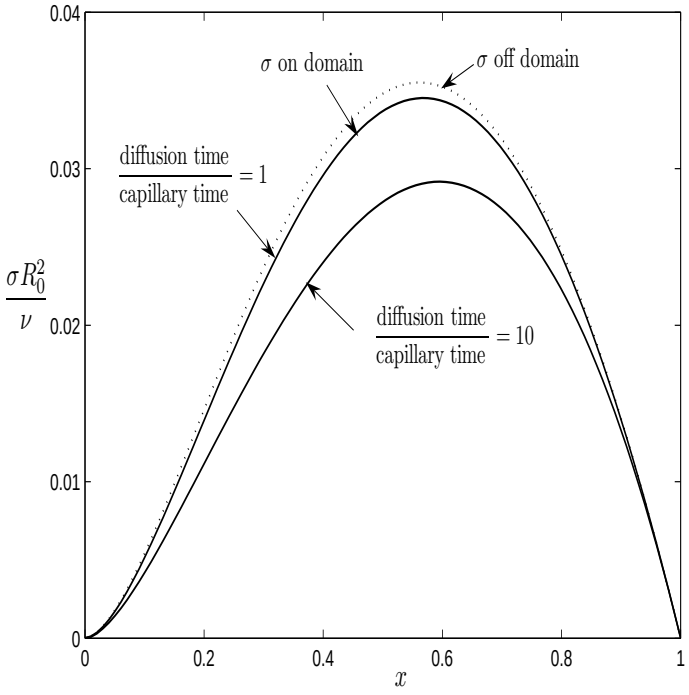


Figure 6: Growth rates for the Navier-Stokes jet

vanish as $x$ approaches zero and the approximation is weaker in the neighborhood of the greatest value of $\sigma$ than it is elsewhere. Third, both $\sigma$ and $\sigma_S$ rise as $x$ increases from zero and $\sigma_S$ always exceeds $\sigma$. And fourth, the inside fluid controls the value of $\sigma$ at small values of $x$.

To understand what we see in these graphs we note that in a flow problem for a crest to grow fluid must flow into the crest. The diameter changes from trough to crest provide the pressure difference for this and $\sigma_S$ exceeds $\sigma$ due to the fact that some of the pressure difference goes to overcome inertia when $\sigma$ is retained on the domain. This effect of $\sigma$ on the domain differs from that observed in phase change or diffusion problems. As $x$ increases from zero the diameter effect on the pressure difference does not change but the pressure gradient increases increasing $\sigma$ and $\sigma_S$. This rise slows and reverses as the effect of longitudinal curvature on the pressure difference increases in importance.

The jet is not unstable at $x = 0$, neither by $\sigma$ nor $\sigma_S$, due to the fact that while the pressure difference remains, the pressure gradient vanishes as the wave length of the disturbance increases.

There are two afterthoughts worth bringing to the readers attention. They both have to do with a jet in absence of an outside fluid, i.e., $\mu^* = 0 = \rho^*$. First, Rayleigh's view of this problem was drawn from his formula for the case $\mu^* = 0 = \rho^*$ and also $\rho = 0$, i.e.,

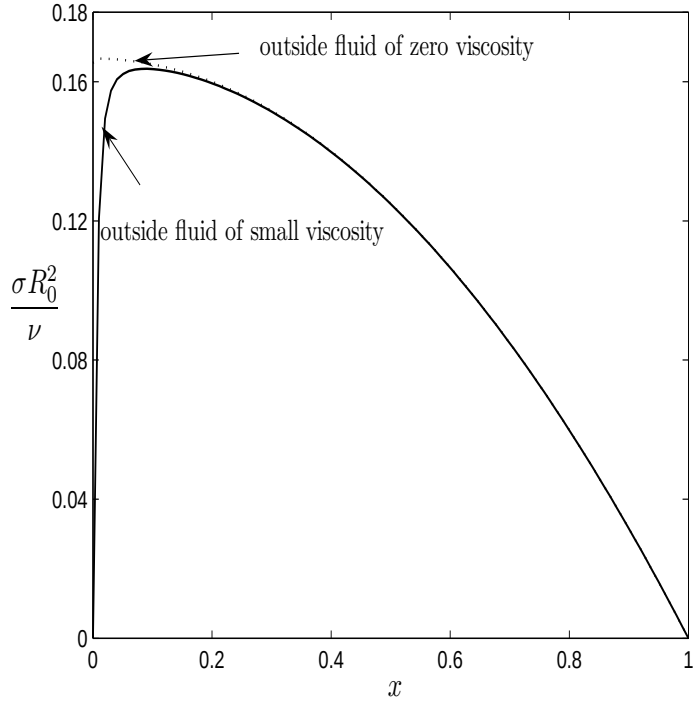


Figure 7: The effect of small viscosity of an outside fluid on $\sigma_S$

dominant viscosity, which shows the greatest growth rate shifting to the left and coming to rest at $x = 0$, $\sigma_S > 0$. This led to Rayleigh's speculation that a viscous jet would breakup at few and distant places, no regular pattern being observable. What is interesting is that, if $\rho = 0 = \rho^*$ but a little surrounding viscosity is added, viz., a jet in air, then $\sigma_S$ approaches zero as $x$ goes to zero and a maximum growth rate at a finite $x$ will be seen. But this will not invalidate Rayleigh's conclusion as the graph in Fig. 7 shows. The rise from zero is very strong and the curve is not easily distinguished from Rayleigh's curve. Perhaps, then, Rayleigh's conclusion survives this test.

Second, Taylor 1934 [6] observed the breakup of jets in regular patterns using two fluids of nearly the same viscosity. Setting $\rho = 0 = \rho^*$, Tomotika 1935 [7] presented growth curves agreeing with Taylor's observation. To see if such a pattern could have been predicted with $\mu^* = 0 = \rho^*$ but now retaining $\rho > 0$ we present Fig.8 where now the rise is due to the inertia of the jet, not the viscosity of the surrounding fluid.

It appears that taking density into account is nearly as good a way to account for Taylor's observation as taking the viscosity of the surrounding fluid into account. To estimate the wavelength at maximum growth rate Tomotika needed to know only the value of $R_0$, which he estimated to be about 1/4 mm. We need this and also some hard to estimate physical properties such as the surface tension.

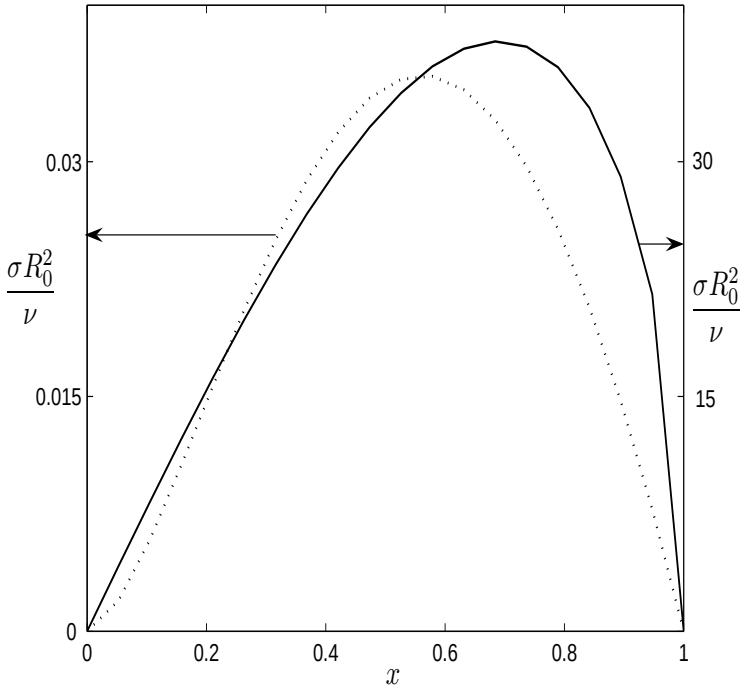


Figure 8: Growth rates when an outside viscous fluid surrounds the inside jet. Tomotika's model for surface dynamics, left, is compared with the one-fluid model with domain dynamics, right

# 5 Conclusion

Our aim is to present a simple experiment where one can easily obtain an instability and then easily learn something about a problem from observation.

To observe an instability one can do no better than run an experiment in a cylindrical geometry. No matter the system the instability occurs for the same reason, viz., cylinders are doubly curved surfaces with the two curvatures having opposing effects on the growth rate of a displacement.

To most easily learn something by observing an instability the simplest thing to do is to run an equilibrium experiment, but of course, this is true because we have already chosen a cylindrical geometry. For example in electrodeposition both the surface tension and the exchange current density are input variables whose values are difficult to estimate. These values could be derived from equilibrium experiments on cylindrical electrodes.

To interpret such experiments, it would be far easier to use the formulas for $\sigma_S$ than it would be to use the formula for $\sigma$. Hence, in the paper we indicate where $\sigma_S$ ought to be a good approximation to $\sigma$ and we explain the different physics at work in phase change

problems versus flow problems.

# References

[1] J. Bockris, A. Reddy. Modern electrochemistry, Vol.1, 2. Plenum Press, New York, 1970.

[2] S. Chandrasekhar. Hydrodynamic and hydromagnetic stability. Clarendon press, Oxford, 1961.

[3] W.W. Mullins, R.F. Sekerka. *Stability of a planar interface during solidification of a dilute binary alloy.* J. Appl. Phys. 35 (1964), 444-451.

[4] J.W.S. Rayleigh. *On the capillary phenomena of jets.* Proc. Roy. Soc., 29 (1879), 71-97.

[5] L. Sundström, F. Bark. *On morphological instability during electrodeposition with a stagnant binary electrolyte.* Electrochim. Acta, 40 (1995), 599-614.

[6] G.I. Taylor. *The Formation of emulsions in definable fields of flow.* Proc. Roy. Soc. Lond. A., 146 (1934), No. 858, 501-523.

[7] S. Tomotika. *On the instability of a cylindrical thread of a viscous liquid surrounded by another viscous fluid.* Proc. Roy. Soc. Lond. A, 150 (1935), No. 870, 322-337.

[8] D.J. Wollkind, R.D. Notestine. *A Non-linear stability analysis of the solidification of a pure substance.* IMA J. Appl. Math., 27 (1981), 85-104.